

UC Davis

UC Davis Previously Published Works

Title

Brown Adipose Tissue Improves Whole-Body Glucose Homeostasis and Insulin Sensitivity in Humans

Permalink

<https://escholarship.org/uc/item/6c788903>

Journal

Diabetes, 63(12)

ISSN

0012-1797

Authors

Chondronikola, Maria
Volpi, Elena
Børsheim, Elisabet
et al.

Publication Date

2014-12-01

DOI

10.2337/db14-0746

Peer reviewed

Maria Chondronikola,^{1,2,3,4} Elena Volpi,^{3,5,6,7} Elisabet Børsheim,^{1,8} Craig Porter,^{1,8} Palam Annamalai,⁹ Sven Enerbäck,¹⁰ Martin E. Lidell,¹⁰ Manish K. Saraf,^{1,8} Sebastien M. Labbe,¹¹ Nicholas M. Hurren,^{1,8} Christina Yfanti,^{1,6} Tony Chao,^{1,2,3} Clark R. Andersen,^{1,8} Fernando Cesani,¹² Hal Hawkins,^{13,14} and Labros S. Sidossis^{1,3,4,5,6,7}



Brown Adipose Tissue Improves Whole-Body Glucose Homeostasis and Insulin Sensitivity in Humans

Diabetes 2014;63:4089–4099 | DOI: 10.2337/db14-0746

Brown adipose tissue (BAT) has attracted scientific interest as an antidiabetic tissue owing to its ability to dissipate energy as heat. Despite a plethora of data concerning the role of BAT in glucose metabolism in rodents, the role of BAT (if any) in glucose metabolism in humans remains unclear. To investigate whether BAT activation alters whole-body glucose homeostasis and insulin sensitivity in humans, we studied seven BAT-positive (BAT⁺) men and five BAT-negative (BAT⁻) men under thermoneutral conditions and after prolonged (5–8 h) cold exposure (CE). The two groups were similar in age, BMI, and adiposity. CE significantly increased resting energy expenditure, whole-body glucose disposal, plasma glucose oxidation, and insulin sensitivity in the BAT⁺ group only. These results demonstrate a physiologically significant role of BAT in whole-body energy expenditure, glucose homeostasis, and insulin sensitivity in humans, and support the notion that BAT may function as an antidiabetic tissue in humans.

Diabetes mellitus currently affects 25.8 million Americans (1). Obesity, which typically precedes diabetes, results in altered glucose control. Indeed, adiposity has been implicated in the etiology of insulin resistance, where lipid moieties from the white adipose tissue (WAT) depots disrupt insulin signaling.

Adult humans have recently been shown to have brown adipose tissue (BAT) (2–4). Further, BAT is associated with leanness (5) and euglycemia (4,6,7), suggesting that, unlike other adipose tissue depots, BAT may be protective against obesity and diabetes. The unique feature of BAT that explains the proposed effects on obesity and glucose control is the abundance of mitochondria, which contain uncoupling protein 1 (UCP1). UCP1 uncouples oxidative phosphorylation by allowing protons to re-enter the mitochondrial matrix independent of ATP synthase, producing heat instead of chemical energy (8). Rodent studies show that, upon stimulation, BAT uses glucose and free fatty acids (FFAs) for thermogenesis (8), confirming the regulatory role of BAT in

¹Metabolism Unit, Shriners Hospital for Children, Galveston, TX

²Department of Preventive Medicine and Community Health, University of Texas Medical Branch, Galveston, TX

³Department of Nutrition and Metabolism, Division of Rehabilitation Sciences, University of Texas Medical Branch, Galveston, TX

⁴Department of Nutrition and Dietetics, Harokopio University of Athens, Athens, Greece

⁵Institute for Translational Sciences, University of Texas Medical Branch, Galveston, TX

⁶Sealy Center on Aging, University of Texas Medical Branch, Galveston, TX

⁷Department of Internal Medicine, University of Texas Medical Branch, Galveston, TX

⁸Department of Surgery, University of Texas Medical Branch, Galveston, TX

⁹Department of Interventional Radiology, University of Texas Medical Branch, Galveston, TX

¹⁰Department of Medical and Clinical Genetics, Institute of Biomedicine, The Sahlgrenska Academy, University of Gothenburg, Gothenburg, Sweden

¹¹Quebec Heart and Lung Research Institute Centre, Quebec City, Quebec, Canada

¹²Department of Nuclear Medicine, University of Texas Medical Branch, Galveston, TX

¹³Department of Pathology, University of Texas Medical Branch, Galveston, TX

¹⁴Department of Pathology, Shriners Hospital for Children, Galveston, TX

Corresponding author: Labros S. Sidossis, lasidoss@utmb.edu.

Received 10 May 2014 and accepted 10 July 2014.

Clinical trial reg. no. NCT01791114, clinicaltrials.gov.

This article contains Supplementary Data online at <http://diabetes.diabetesjournals.org/lookup/suppl/doi:10.2337/db14-0746/-/DC1>.

© 2014 by the American Diabetes Association. Readers may use this article as long as the work is properly cited, the use is educational and not for profit, and the work is not altered.

See accompanying article, p. 3998.

adiposity, glucose homeostasis, and insulin sensitivity (9,10).

The physiological significance of BAT activation in whole-body substrate metabolism in humans remains unclear. Orava et al. (11) reported that cold exposure (CE) resulted in a 12-fold increase in glucose disposal in BAT, but not in other tissues. Ouellet et al. (12) reported similar results. This suggests that, upon activation, BAT clears plasma glucose. However, these investigators did not show differences in whole-body insulin-stimulated glucose disposal between individuals with detectable BAT (BAT⁺) or nondetectable BAT (BAT⁻), questioning the ability of BAT to modulate whole-body glucose metabolism. Similarly, Ouellet et al. (12) recently showed that under short-term CE, BAT primarily oxidizes intracellular fatty acids; plasma substrate oxidation by BAT was minimal (12).

The results from the aforementioned studies question the role of BAT in whole-body metabolism in humans. However, Orava et al. (11,13) compared whole-body insulin-stimulated glucose disposal between BAT⁺ and BAT⁻ groups under thermoneutral (TN) conditions. The role of BAT in whole-body glucose metabolism is likely more readily discerned when BAT is activated. Furthermore, Ouellet et al. (12) demonstrated that BAT minimally contributed to whole-body plasma glucose utilization, which might be due to the shorter duration of CE and the presence of mild shivering. Animal studies (8) suggest that BAT first consumes intracellular energy stores before using plasma-borne substrates to support its energy needs. Subsequently, a longer CE may be necessary to elucidate the role of BAT activation in plasma glucose disposal and oxidation in humans.

The aim of this study was to investigate the effect of prolonged (5–8 h) cold-induced BAT activation on the whole-body glucose metabolism. Twelve men (7 BAT⁺ and 5 BAT⁻) were studied under CE and TN conditions. CE increased resting energy expenditure (REE), plasma glucose oxidation, and whole-body insulin-stimulated glucose disposal in the BAT⁺ individuals only. The current data support a physiologically significant role for BAT in whole-body glucose homeostasis and insulin sensitivity in humans.

RESEARCH DESIGN AND METHODS

Subjects

Twelve males participated in the study. The participants were screened for health status, smoking, alcohol or drug use, and recent medication or supplement use. Only healthy individuals qualified to participate in the study. Informed written consent was obtained from all participants prior to their inclusion in the study in accordance with the Declaration of Helsinki. The University of Texas Medical Branch and Institute for Translational Sciences Institutional Review Boards approved the experimental protocol.

Experimental Protocol

Each participant completed one CE study and one TN study, 2 weeks apart (Fig. 1). The CE trial was performed

first to determine BAT volume and anatomical location using 2-deoxy-2-[¹⁸F]-fluoro-D-glucose (¹⁸F-FDG) positron emission tomography (PET)/computed tomography (CT) scanning.

Three days before each study, subjects followed a weight-maintaining diet and refrained from physical activity and the consumption of alcohol and caffeine. The evening before the study, subjects were admitted to the Institute for Translational Sciences-Clinical Research Center at the University of Texas Medical Branch. Patients were fed a standardized evening meal. During CE and TN studies, subjects were fasted overnight and remained rested in bed for the duration of the study. Subjects wore standardized clothing (T-shirt and shorts).

CE Protocol and TN Conditions

We used the following individualized CE protocol to maximize nonshivering thermogenesis; subjects were studied in a room with an ambient temperature of ~19°C and wearing garments cooled by liquid circulation (Cool Flow vest and blanket; Polar Products Inc., Stow, Ohio). The temperature of the vest was initially set at 20°C, then decreased at 1°C intervals through an air-conditioned temperature control bath (Chiller Reservoir System; Polar Products Inc.) until subjects reported shivering. Then the temperature was increased by 1°C and was maintained at a constant temperature. We visually inspected the subjects for shivering. In a subset of individuals ($n = 3$), we performed electromyography (Bagnoli 8; Delsys, Boston, MA) at 5-min intervals to verify muscle activity (14). Core temperature and skin temperature were measured using a telemetric pill (Core-Temp; HQ Inc., Palmetto, FL) and wireless probes (iButtons; Maxim Integrated Products, Dallas, TX) (15), respectively.

Stable Isotope Infusion

After 3 h of either the CE or the TN study, blood was sampled to determine background enrichment, prior to the administration of the following stable isotope tracers (Cambridge Isotope Laboratories, Andover, MA) through a catheter in the forearm vein, as follows: 1) a primed (17.6 μmol/kg), constant (0.22 μmol/kg/min) 2-h infusion of [6,6-²H₂]-glucose to assess glucose kinetics (16); 2) a constant 2-h infusion of potassium [U-¹³C₁₆]-palmitate (0.02 μmol/kg/min) to assess FFA kinetics (17,18); and 3) a bolus of NaH¹³CO₃ (55 μmol/kg dissolved in 0.9% NaCl) was also given to prime the body's bicarbonate pool. Blood and breath samples were obtained at 1 h and 50 min, 1 h and 55 min, and 2 h after the initiation of the stable isotope infusion to determine isotopic enrichments of plasma glucose and palmitate, and breath CO₂, and to measure substrate concentrations. The same regimen, including only [6,6-²H₂]-glucose, was repeated during the hyperinsulinemic-euglycemic clamp. Whole-body glucose disposal and FFA oxidation were calculated as previously described (19,20). Changes between CE and TN in glucose uptake were calculated as the difference between the glucose uptake in CE and TN conditions.

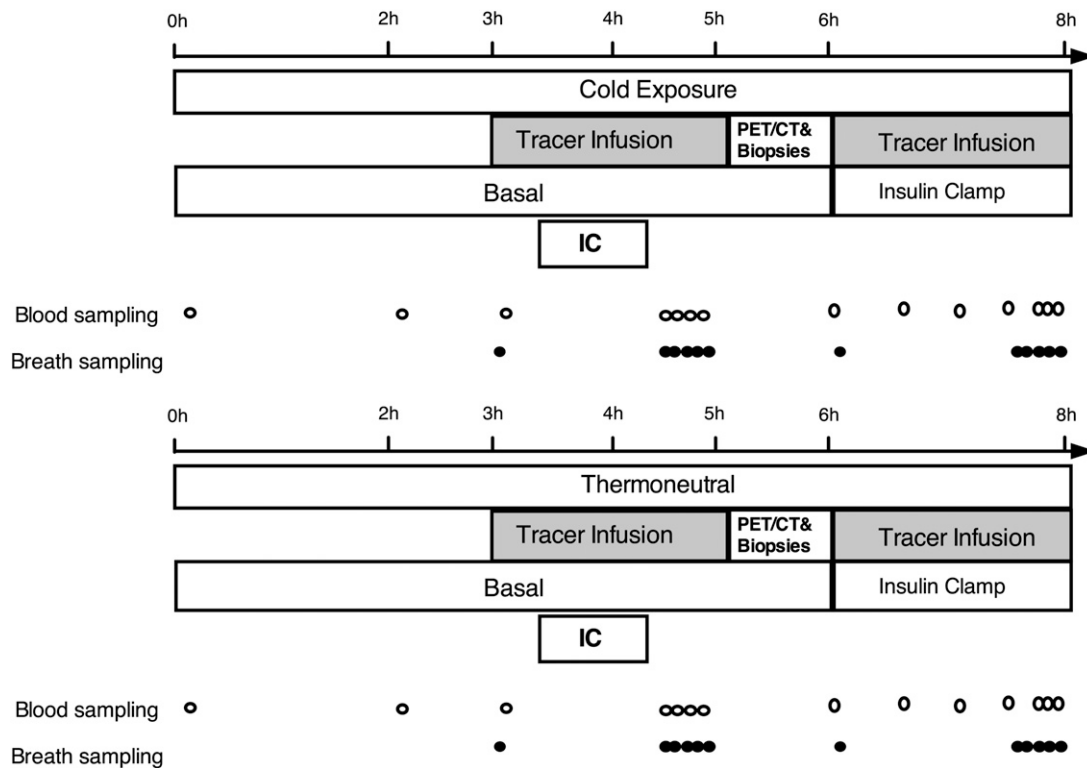


Figure 1—Study design. The following tracers infused: [6,6- $^2\text{H}_2$]-glucose, [U- $^{13}\text{C}_{16}$] palmitate, and ^{13}C sodium bicarbonate. IC, indirect calorimetry.

Hyperinsulinemic-Euglycemic Clamp

Hyperinsulinemic-euglycemic clamps were conducted during the last 2 h of each trial, as previously described (21). Insulin (Lilly, Indianapolis, IN) was administered at a rate of 20 mU/m²/min, dissolved in sterile NaCl 0.9% (19). We used a low insulin infusion rate to avoid the stimulation of muscle plasma glucose disposal (22). Whole-body insulin-stimulated glucose disposal was evaluated using the insulin sensitivity index (23) and the following formula: glucose disposal (in micromoles per kilogram per minutes)/steady-state plasma glucose (in milligrams per deciliter) (24).

PET/CT Scanning

After 5 h, subjects were injected with a bolus of 185 MBq ^{18}F -FDG. We performed a PET/CT scan (GE Discovery ST 4 Slice scanner; General Electric, Milwaukee, WI) an hour later to assess BAT volume and BAT glucose disposal (BAT volume [in milliliters] \times mean standardized disposal value [SUV; in grams per milliliter]). An independent blinded investigator assessed the PET/CT scans for BAT, as previously described (12). Subjects with pronounced ^{18}F -FDG disposal were assigned to the BAT⁺ group ($n = 7$; BAT volume 69 ± 18 mL) (Supplementary Fig. 1), while subjects with no or minimal ^{18}F -FDG disposal were assigned to the BAT⁻ group ($n = 5$; BAT volume 4.4 ± 2.3 mL; $P < 0.05$) (Supplementary Fig. 2).

Body Composition

DEXA (Lunar iDXA*; GE Healthcare, Mickleton, NJ) was used to evaluate the lean and fat body mass of the

participants. CT was used to estimate total, subcutaneous, and visceral abdominal tissue area (25–27).

Indirect Calorimetry

REE was calculated using whole-body oxygen consumption and carbon dioxide production rates measured by indirect calorimetry (Vmax Encore; CareFusion Corporation, San Diego, CA) (28). Indirect calorimetry equipment failed on two occasions (one BAT⁺ subject and one BAT⁻ subject).

Blood Samples Analysis

Plasma glucose concentrations were determined using an automated glucose analyzer (Stat 2300; Yellow Spring Instruments). Gas chromatography mass spectrometry was used to quantify plasma enrichments of glucose and palmitate (Agilent, Santa Clara, CA). Plasma insulin and free triiodothyronine (FT3) concentrations were measured using chemiluminescence (Dxi 600 analyzer; Beckman Coulter, Pasadena, CA). Free thyroxine (FT4) was measured via a quantitative electrochemiluminescent immunoassay (ARUP, Salt Lake City, UT). Plasma norepinephrine level was determined using quantitative high-performance liquid chromatography (ARUP, Salt Lake City, UT). Further, serum interleukin-6 (IL-6) (R&D Systems, Minneapolis, MN), plasma irisin (Phoenix Pharmaceuticals, Burlingame, CA), and fibroblast growth factor 21 (FGF21) (BioVendor, Asheville, NC) concentrations were determined using commercially available ELISA kits.

Adipose Tissue Sampling

During CE, adipose tissue samples from the supraclavicular and abdominal areas were obtained using a Bergström needle. In a subset of individuals (three BAT⁺ and one BAT⁻ individuals), biopsy samples were obtained during both the CE and TN trials. The location for the supraclavicular biopsy was determined by the ¹⁸F-FDG PET/CT scan images showing cold-activated BAT. In BAT⁻ individuals, the supraclavicular depot was sampled 2–3 cm from the skin surface area, which is the same depth that the BAT depot has been localized in BAT⁺ individuals. Each sample was divided into pieces for the analyses described below.

Immunohistochemistry

Adipose tissue, preserved in 10% formalin, was embedded in paraffin wax. Immunohistochemistry was performed using a standard protocol (29). Briefly, after blocking (Rabbit IgG kit; Vector Laboratories, Burlingame, CA) for 45 min, sections were incubated overnight with primary antibody (1:1,600, rabbit anti-UCP1 antibody, U6382; Sigma-Aldrich) at 4°C. Sections were incubated with secondary antibody (rabbit IgG; Vector Laboratories), ABC solution, and then a diaminobenzidine solution (DAB peroxidase substrate kit; Vector Laboratories) at room temperature.

Mitochondrial Respiration

Mitochondrial function was determined by high-resolution respirometry (30). Briefly, maximal uncoupled mitochondrial respiration was measured in permeabilized (5 μmol/L digitonin) WAT (~50 mg) and BAT (~10 mg) after the addition of substrates (1.5 mmol/L octanoyl-carnitine, 5 mmol/L pyruvate, 10 mmol/L glutamate, 2 mmol/L malate, 5 mmol/L ADP, and 10 mmol/L succinate) and the ATP synthase inhibitor oligomycin (5 μmol/L).

Gene Expression

Total RNA was isolated, and cDNA was synthesized and analyzed by quantitative real-time PCR, as previously described (2), using gene-specific primers at a final concentration of 300 nmol/L (Supplementary Table 2). 18S was used as the normalizing gene and an established supraclavicular BAT sample was included as a positive control for BAT (2).

Statistical Analysis

Results are presented as means ± SEM/SD. Differences between CE and TN trials were evaluated using paired *t* tests for normally distributed data. Non-normally distributed data were evaluated using a Wilcoxon rank sum test. A one-sample *t* test was used to evaluate whether CE induced changes in the various metabolic measurements compared with TN. Differences between BAT⁻ and BAT⁺ subjects were evaluated using a Mann-Whitney *U* test.

To evaluate differences in the circulating levels of the various hormones/cytokines, we used a mixed ANOVA model. Treatment differences (CE-TN) in the levels of hormones/cytokines were determined for each subject at

each time point, accounting for the paired within-subject correlation between treatments. A mixed ANOVA modeled the differences as a function of time and BAT status, an autoregressive model of order 1 correlation structure accounted for by the within-subject repeated measures over time, and a weighting structure adjusted for heterogeneity of variance over time. Differences were transformed as needed to better approximate normal distributions, with results inverse transformed appropriately. Statistical analyses were performed using GraphPad, version 5 (GraphPad Software, La Jolla, CA) for the Mac OS X operating system and R statistical software (R Core Team, 2013, version 3.0.1). All statistical tests assumed a 95% level of confidence.

RESULTS

By design, the BAT⁺ group had higher BAT volume and activity ($P < 0.05$) than the BAT⁻ group, but they were similar in age and anthropometric characteristics (Table 1). BAT⁺ individuals required slightly, but not significantly, lower ambient and garment temperatures to reach their nonshivering threshold (Supplementary Table 1). CE decreased skin temperature in both groups ($P < 0.05$). The BAT⁻ group had a marginally lower core temperature during CE conditions compared with that during TN conditions ($P = 0.06$).

BAT Activation Increases Energy Expenditure and Plasma Substrate Oxidation

Indirect calorimetry and stable isotopes were used to determine REE and substrate oxidation rates. CE increased REE (15%) in the BAT⁺ group only ($P < 0.05$) (Fig. 2A), suggesting that BAT activation increases REE during nonshivering CE. The cold-induced increase in REE in the BAT⁺ group was fueled primarily by plasma-derived glucose and FFA oxidation ($P < 0.05$ for both) (Fig. 2B and C). Plasma glucose and FFA contributed ~30% and 70%, respectively, to the observed increase in REE in the BAT⁺ group. These data suggest that, upon prolonged stimulation, BAT largely oxidizes plasma substrates to support its energy demands. This finding supports a role for BAT in the regulation of systemic glucose and FFA metabolism.

Glucose Disposal During CE Occurs Primarily in BAT

¹⁸F-FDG uptake during CE increased significantly in BAT ($P < 0.05$), but not in the liver, abdominal visceral adipose tissue, abdominal subcutaneous adipose tissue, or skeletal muscle (vastus lateralis and pectoralis) (Fig. 3). Interestingly, the mean heart SUV decreased significantly with CE in BAT⁺ subjects ($P < 0.05$). In agreement with previous reports (11,12), our data suggest that mild CE results in increased disposal of labeled glucose by BAT only, with minimal or no effects in other tissues.

BAT Activation Increases Basal Whole-Body Glucose Disposal

To determine the physiological significance of BAT activation on whole-body glucose metabolism, we assessed glucose

Table 1—Subject characteristics

Parameters	BAT ⁻ (n = 5)	BAT ⁺ (n = 7)
Age (years)	49.8 ± 7.3	41.2 ± 5.3
BMI (kg/m)	30.0 ± 2.8	28.2 ± 1.5
BSA (m ²)	2.1 ± 0.1	2.0 ± 0.1
Lean mass (kg)	58.8 ± 3.4	58.3 ± 3.7
Body fat (%)	32.3 ± 22.7	31.3 ± 3.2
Visceral adipose tissue (cm ²)	57.8 ± 12.2	41.9 ± 8.4
Subcutaneous adipose tissue (cm ²)	90.0 ± 22.7	94.3 ± 12.0
BAT volume (mL)	4.4 ± 2.3	69.0 ± 18.0*
BAT activity (BAT volume [mL] × mean SUV [g/mL])	9.3 ± 4.4	153.2 ± 42.6*
AUC _{glu} (mg/dL)	296.3 ± 15.6	248.5 ± 25.6

Data are mean ± SEM. AUC_{glu}, glucose area under the curve; BSA, body surface area. *P < 0.05.

kinetics during TN conditions and during prolonged (5 h) CE. CE significantly increased whole-body glucose disposal only in the BAT⁺ group ($P < 0.05$) (Table 2, Fig. 4A). Theoretically, if BAT remained chronically active, it could dispose ~23 g of glucose in 24 h. Combined with the PET/CT scan data, showing that ¹⁸F-FDG uptake increased only in BAT (Fig. 3), these data suggest that, when activated, BAT has the ability to take up significant amounts of glucose from the circulation, and therefore can play a significant role in glycemic control.

BAT Activation Increases Insulin-Stimulated Whole-Body Glucose Disposal

Under thermoneutrality, insulin infusion significantly increased whole-body glucose disposal in both groups ($P < 0.05$ for both) (Table 2). This increase reflects increased glucose disposal in many tissues and indicates that the two groups were sensitive to insulin in peripheral tissues (i.e., skeletal muscle, WAT), even though the BAT⁻

group needed higher insulin levels to achieve the same result (i.e., slightly less insulin sensitive). Further, insulin infusion suppressed endogenous glucose production similarly in both groups ($P < 0.05$), indicating that both groups were sensitive to insulin at the level of the liver.

After establishing that both groups were responsive to insulin, we determined the effect of cold-induced BAT activation on glucose disposal during hyperinsulinemia (resembling the postprandial state). To this end, we infused insulin after 6 h of CE. Compared with the insulin-induced increase in glucose disposal in thermoneutrality, CE further increased glucose disposal in the BAT⁺ group only ($P < 0.05$) (Table 2, Fig. 4B). The results were similar when the whole-body glucose disposal rates were corrected for glucose levels (whole-body insulin sensitivity index) (Fig. 4C) or in combination with insulin concentration (insulin sensitivity index) (Fig. 4D). Finally, hyperinsulinemia equally suppressed endogenous glucose production in both groups under CE conditions ($P < 0.05$). These findings suggest that BAT activation may play a functional role in peripheral glucose disposal, both in the postabsorptive and postprandial state.

BAT Status and Hormonal/Cytokine Response to Cold

Our study was not designed to examine the mechanisms regulating the effect of BAT activation on glucose metabolism. Nevertheless, we measured the levels of FT3, FT4, FGF21, cytokines (irisin, leptin, IL-6), and norepinephrine, which have been previously associated with BAT activation (8,10,30,31). The BAT⁺ group demonstrated higher increases in the circulating concentrations of norepinephrine, FGF21, and FT3, when compared with the BAT⁻ group (Fig. 5A–C). FT4, irisin, and IL-6 levels were not significantly different between the two groups (Fig. 5D–F).

Molecular and Functional Characterization of BAT

The assignment of subjects into the BAT⁺ and BAT⁻ groups was based on the cold-induced glucose uptake in the supraclavicular region as assessed by PET/CT scanning. The reason for the low supraclavicular glucose

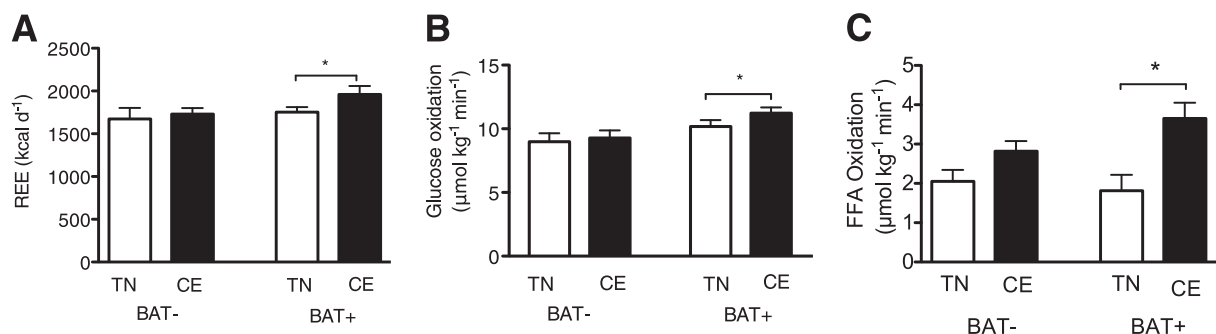


Figure 2—The role of BAT in REE and substrate oxidation. A: REE upon CE and TN conditions in BAT⁺ subjects and BAT⁻ subjects. B: Plasma glucose oxidation under CE and TN conditions in BAT⁺ and BAT⁻ subjects. C: Plasma FFA oxidation under CE and TN conditions in BAT⁺ and BAT⁻ subjects. White bars, TN; black bars, CE. Data are mean ± SEM. *P < 0.05, CE vs. TN.

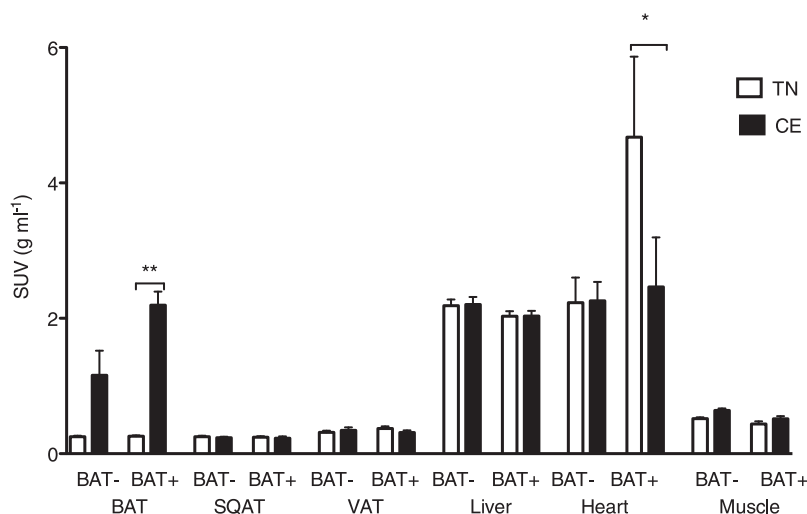


Figure 3—Mean SUV for glucose of various tissues during CE and TN conditions. SQAT, subcutaneous adipose tissue; VAT, visceral adipose tissue; white bars, TN; black bars, CE. Data are mean \pm SEM. * $P < 0.05$, ** $P < 0.01$, CE vs. TN.

uptake in the BAT⁻ group could be due to the fact that this group had less BAT. Alternatively, the BAT⁻ group might have had comparable amounts of BAT, relative to the BAT⁺ group, but was unable to activate it in response to the cold stimulus used (i.e., their threshold for cold-induced activation of BAT may have not been reached). To address the question of whether BAT⁻ subjects had BAT or not, we performed molecular and functional studies on adipose tissue samples collected from the supraclavicular depot by the guidance of the PET/CT scan images, and compared them with abdominal subcutaneous adipose tissue samples.

BAT⁺ subjects had UCP1-positive multilocular adipocytes in the supraclavicular tissue (Fig. 6A), whereas the corresponding tissue of the BAT⁻ subjects demonstrated minimal UCP1 staining and was composed of largely unilocular adipocytes (Fig. 6B). The abdominal subcutaneous adipose tissue samples were similar between the two

groups, comprising unilocular adipocytes with no UCP1 staining (Fig. 6C and D). Quantification of the UCP1 staining confirms these results (supraclavicular adipose tissue BAT⁺ vs. BAT⁻, $P = 0.06$) (Fig. 6E). In agreement with the results from the immunohistochemical analysis, *UCP1* gene expression was higher in the supraclavicular adipose tissue from the BAT⁺ group relative to the BAT⁻ group ($P = 0.06$) (Fig. 6F) and at a similar level as in a well-documented BAT control sample included in the analysis. No *UCP1* expression was detected in the abdominal subcutaneous adipose tissue samples. The molecular studies were complemented with functional studies showing that the maximal uncoupled mitochondrial respiration was significantly higher in the supraclavicular adipose tissue compared with the subcutaneous abdominal adipose tissue ($P < 0.05$) only in the BAT⁺ group (Fig. 6G). These results show that only the supraclavicular adipose tissue from the BAT⁺ group presents with features of BAT,

Table 2—Indices of whole-body glucose homeostasis under CE and TN conditions

Parameters	BAT ⁻ (n = 5)		BAT ⁺ (n = 7)	
	TN	CE	TN	CE
Basal conditions				
Glucose (mg/mL)	90.0 \pm 7.9	94.0 \pm 3.4	93.4 \pm 2.0	89.5 \pm 3.2
Whole-body glucose disposal (μ mol/kg/min)	9.4 \pm 0.7	9.7 \pm 0.6	10.2 \pm 0.5	11.6 \pm 0.2*
Insulin (μ U/mL)	8.6 \pm 4.0	8.2 \pm 1.3	3.9 \pm 0.8†	3.8 \pm 1.0†
Hyperinsulinemic-euglycemic conditions				
Glucose (mg/mL)	83.8 \pm 3.1	85.8 \pm 3.5	81.1 \pm 3.3	81.5 \pm 5.8
Whole-body glucose disposal (μ mol/kg/min)	12.4 \pm 2.2‡	12.8 \pm 1.8	13.0 \pm 0.9‡	16.5 \pm 1.1*,‡
Endogenous glucose production (μ mol/kg/min)	5.6 \pm 1.6	7.5 \pm 1.1	5.3 \pm 1.7	6.3 \pm 1.3
Suppression of endogenous glucose production (%)	-59.7 \pm 9.4	-48.2 \pm 6.9	-62.4 \pm 12.5	-59.1 \pm 9.1
Insulin (μ U/mL)	33.5 \pm 4.3	31.0 \pm 6.7	18.2 \pm 2.0†	18.8 \pm 2.0

Data are mean \pm SEM. * $P < 0.05$, CE vs. TN conditions. † $P < 0.05$, BAT⁻ vs. BAT⁺ subjects. ‡ $P < 0.05$, basal vs. hyperinsulinemic-euglycemic conditions.

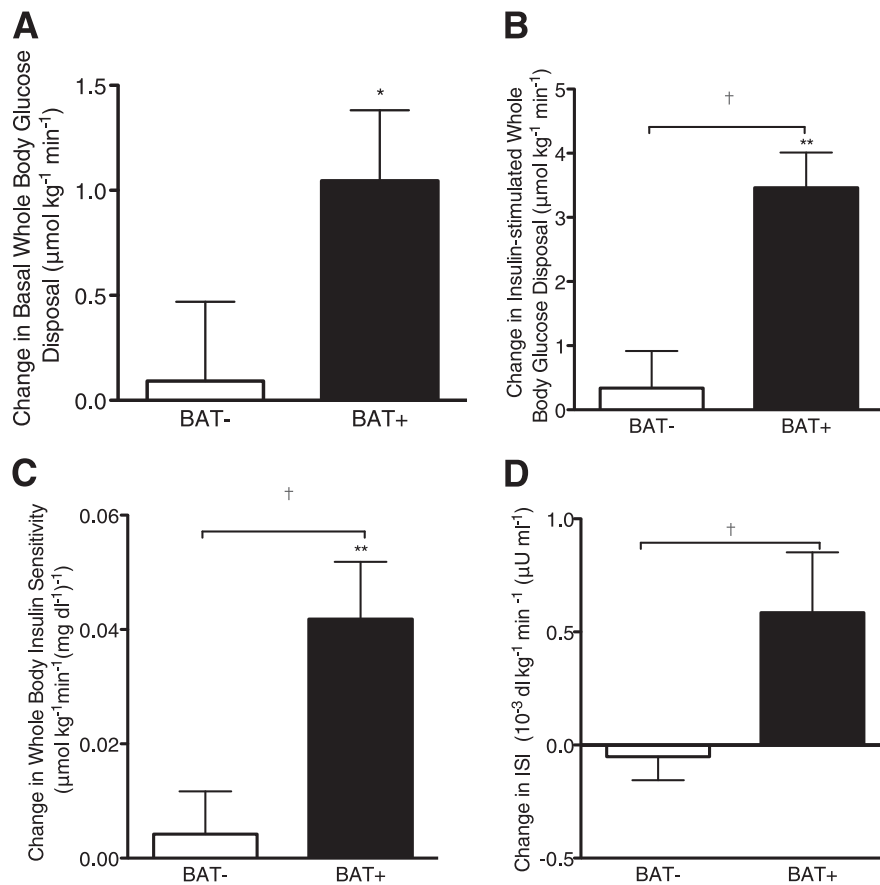


Figure 4—Effect of BAT on whole-body glucose disposal and insulin sensitivity. Change in whole-body glucose disposal under CE relative to TN in basal condition (A) and during hyperinsulinemic-euglycemic clamp (B). C: Change in the insulin sensitivity index (ISI) for CE and TN. D: Change in whole-body insulin sensitivity for CE relative to TN. Data are means \pm SEM. White bars, BAT⁻; black bars, BAT⁺. * $P < 0.05$ and ** $P < 0.01$, significant change with CE vs. TN conditions. † $P < 0.05$, BAT⁺ vs. BAT⁻.

whereas this is not the case for the BAT⁻ group. Hence, the low glucose uptake in the BAT⁻ group is due to a lower BAT content rather than a failure to activate BAT.

To further examine how CE affects human BAT on a molecular level, biopsy samples were taken under both TN and CE conditions in a subset of BAT⁺ subjects. As predicted by animal studies on bona fide BAT, CE induced the expression of both *UCP1* and *DIO2* (type 2 deiodinase) (Fig. 6H and I). In addition, CE induced the expression of *ADRB3* (β 3-adrenergic receptor) and *PGC1 α* (peroxisome proliferator-activated receptor γ coactivator 1 α) (Supplementary Figs. 3 and 4). Hence, CE appears to trigger the expression of essential thermogenic genes in humans. The expression of the *GLUT1* gene increased with CE in three of four subjects, while *GLUT4* gene expression increased in two of four participants (Supplementary Figs. 5 and 6).

DISCUSSION

We have shown a physiologically significant effect of BAT activation on whole-body glucose disposal in humans, supporting a functional role of BAT in glucose homeostasis and insulin sensitivity in humans. Our data suggest

that ~ 70 mL of active BAT can clear significant amounts of glucose from the circulation. This glucose is used to support the cold-induced increase in REE in the BAT⁺ group. Further, this was accompanied by an increase in peripheral insulin-stimulated glucose disposal in BAT⁺ individuals. Our data demonstrate a significant role for BAT activation in altering glucose control and insulin sensitivity in humans.

Plasma glucose oxidation accounted for $\sim 30\%$ of the estimated increase in REE during CE in BAT⁺ subjects. This estimate is consistent with results from animal studies (32). Plasma FFA oxidation was responsible for the remaining 70% of the increase in REE. This is also in agreement with animal data suggesting that FFAs represent the primary substrate oxidized by UCP1-positive mitochondria (32). Our findings of significant plasma substrate use by BAT upon activation are in contrast with a recent report that BAT uses mainly intracellularly stored triacylglycerols and very few, if any, plasma substrates (12). This may be due to the short (2.5 h) duration of CE in this study (12) compared with that in our longer CE protocol (5 h). This supposition is supported by rodent data, which indicate that BAT first exhausts

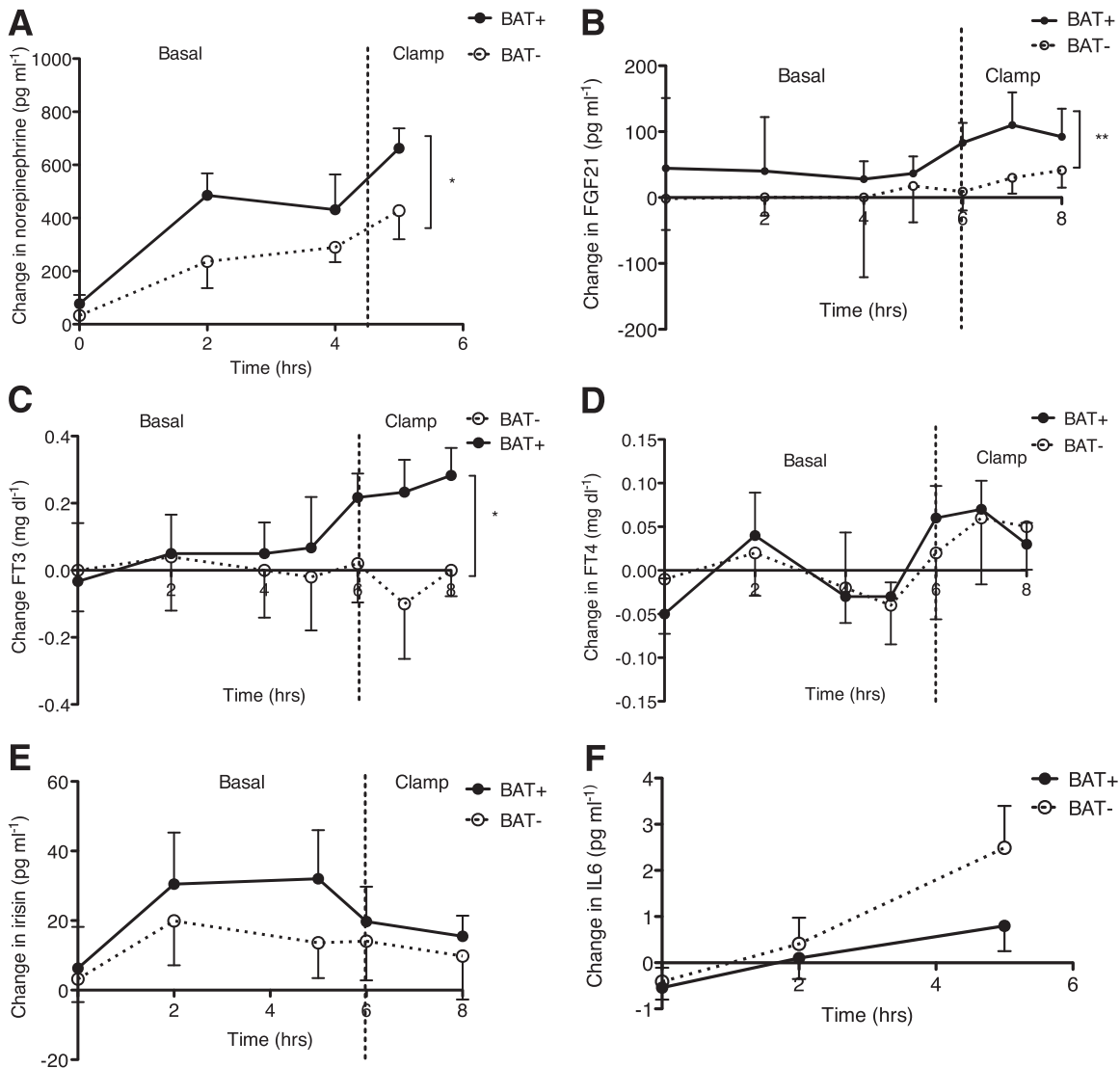


Figure 5—Change in plasma concentrations of hormones and cytokines with CE in BAT⁺ and BAT⁻ subjects. *A*: Change in plasma norepinephrine levels with CE in BAT⁺ and BAT⁻ individuals. *B*: Change in plasma FGF21 concentrations with CE in BAT⁺ and BAT⁻ individuals. Change in plasma FT3 (*C*) and plasma FT4 (*D*) concentrations with CE in BAT⁺ and BAT⁻ individuals. *E*: Change in plasma irisin concentration with CE in BAT⁺ and BAT⁻ individuals. *F*: Change in serum IL-6 concentrations with CE in BAT⁺ and BAT⁻ individuals. Data are mean \pm SEM. * $P < 0.05$ and ** $P < 0.01$, significant difference in response to CE between BAT⁺ and BAT⁻ subjects.

intracellular stores before relying on plasma-borne substrates to support its energy needs (8). Therefore, we believe that our results differ from those previously reported (12) due to our CE protocol being two times longer. The duration of CE should be a consideration for future studies aimed at elucidating the role of BAT activation in human metabolism.

BAT is an insulin-sensitive tissue (11). Moreover, because humans spend a significant portion of the day in the postprandial state, we examined the effect of cold-induced BAT activation during a hyperinsulinemia-euglycemia clamp to simulate the postprandial state in a laboratory setting. Hyperinsulinemia significantly increased whole-body glucose disposal and insulin sensitivity in the BAT⁺ group only. These results suggest that BAT activation may

modulate whole-body glucose metabolism in the postprandial state. Moreover, relative to the TN study, CE improved indexes of insulin sensitivity in the BAT⁺ group only, further supporting a role for BAT activation in whole-body insulin sensitivity in humans.

Although we cannot exclude the contribution of indirect pathways in the observed increase in the insulin-stimulated whole-body glucose uptake, we believe that the increase was due to BAT activation and not a systemic response to CE. This is supported by the fact that hyperinsulinemia during thermoneutrality increased whole-body glucose uptake equally in both groups, whereas hyperinsulinemia during CE increased glucose uptake only in the BAT⁺ group. Moreover, we performed a low-dose insulin clamp to avoid significant muscle glucose uptake. Further, it is unlikely

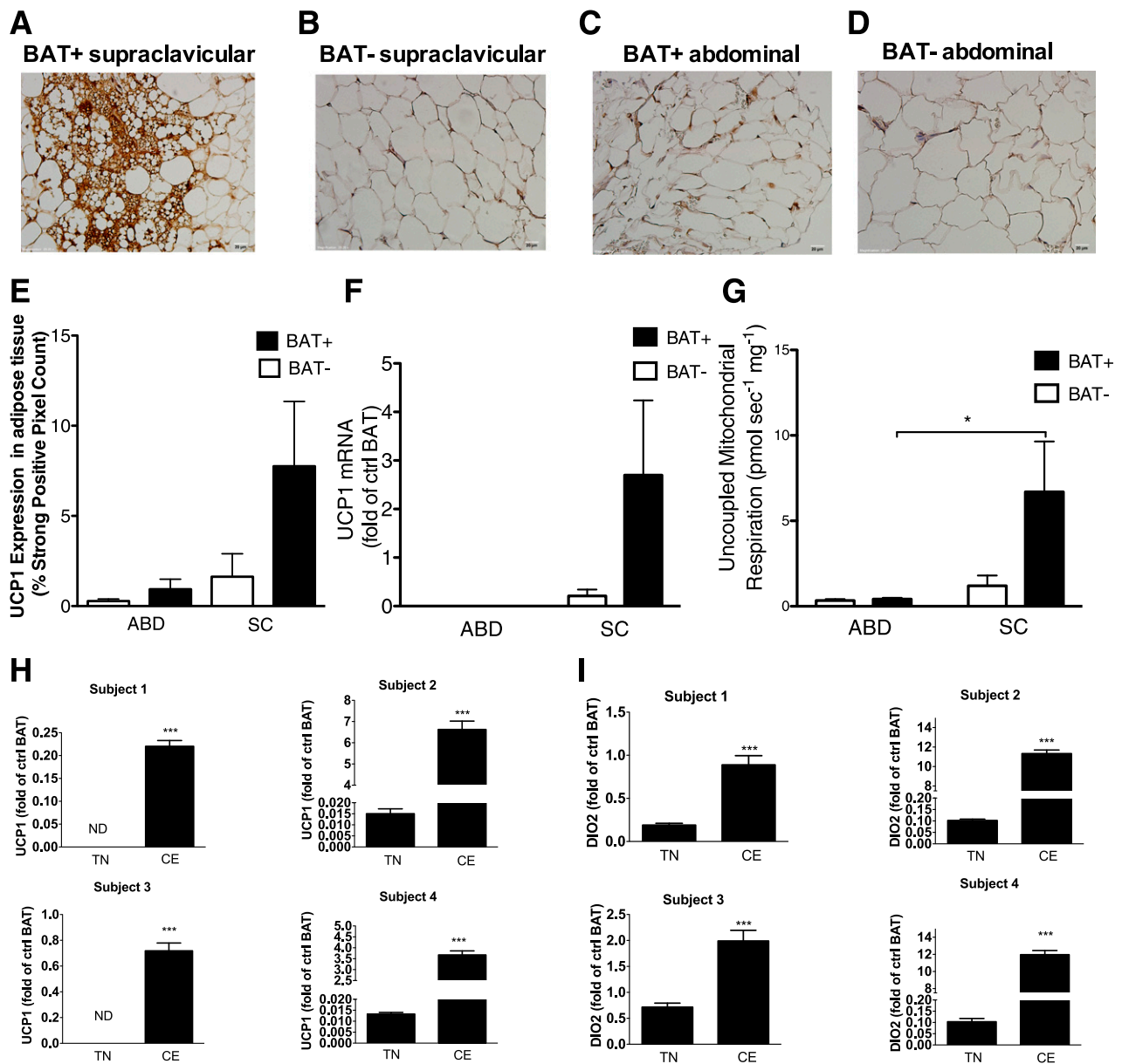


Figure 6—Molecular and functional characterization of supraclavicular and abdominal subcutaneous adipose tissue samples in BAT⁺ and BAT⁻ subjects under conditions of cold-induced BAT. UCP1 staining ($\times 40$) in the supraclavicular (A and B) and abdominal (ABD) subcutaneous (C and D) adipose tissue samples from representative BAT⁺ (A and C) and BAT⁻ (B and D) participants. E: Quantification of UCP1 staining in supraclavicular (SC) and ABD subcutaneous adipose tissue. F: UCP1 gene expression in SC and ABD subcutaneous adipose tissue. G: Uncoupled mitochondrial respiration in SC and ABD subcutaneous adipose tissue. Data are mean \pm SEM. White circles, BAT⁻; black circles, BAT⁺. * $P < 0.05$. H: UCP1 gene expression in BAT under TN and CE conditions. Data are mean \pm SD. *** $P < 0.005$. I: DIO2 gene expression in BAT under TN and CE conditions. Data are mean \pm SD. *** $P < 0.005$.

that muscle glucose uptake was proceeding at a significant rate, as CE causes peripheral vasoconstriction (33), which has been shown to decrease peripheral insulin-stimulated glucose uptake (34). Indeed, CE has been found to preferentially enhance insulin signaling in BAT, and to perturb insulin signaling in muscle and WAT (35), suggesting that BAT is likely the tissue primarily responsible for the reported improvements in insulin sensitivity during CE.

Norepinephrine also induces BAT activation by causing lipolysis (8). FFAs subsequently bind to and activate UCP1, leading to mitochondrial thermogenesis (8). We observed greater norepinephrine levels in response to CE in the BAT⁺ subjects, which was likely responsible for the increase in REE observed in the BAT⁺ group. Moreover, norepinephrine production can stimulate BAT to produce FGF21 (36). FGF21 improves glucose homeostasis

and insulin sensitivity by increasing *GLUT1* expression in WAT. A number of animal studies (8,10) and a few recent humans studies support a role for BAT as an endocrine tissue (37). In agreement with this, CE induced greater increases in circulating levels of FT3, norepinephrine, and FGF21 in the BAT⁺ group compared with the BAT⁻ group in the current study. Thus, the reported improvement in insulin sensitivity in BAT⁺ subjects may be attributable to circulating levels of FGF21 during CE. Adrenergic stimulation and FT3 are upstream regulators of FGF21 production. Therefore, the concomitant increase in FT3 and norepinephrine levels highlights a plausible pathway by which BAT may function as an endocrine organ. Specifically, CE increases *DIO2* activity in BAT, resulting in an acceleration in the conversion of thyroxine to triiodothyronine, the active form of thyroid hormone (38). Indeed, our results also show increased *DIO2* expression in BAT upon CE. In mice, triiodothyronine stimulates the sympathetic nervous system, leading to higher *UCP1* expression in BAT (30).

The strengths of this study include the use of an individualized, prolonged nonshivering CE protocol to elicit maximal nonshivering thermogenesis and BAT activation, along with the use of gold standard direct measures of whole-body glucose metabolism in individuals with or without active BAT depots. Although the methodological approaches available and the restrictions governing human research limit our ability to provide more direct and mechanistic evidence, the results of this study strongly support the idea that BAT activation plays a physiologically significant role in whole-body glucose and energy metabolism in humans. The use of invasive methodologies to directly measure substrate metabolism and collect supraclavicular biopsy samples from human volunteers allow physiologically meaningful conclusions to be made.

In conclusion, our results suggest that BAT activation increases whole-body glucose disposal and insulin sensitivity in humans. These results support a functional role of BAT in whole-body glucose and energy homeostasis. Future research is needed to further investigate the effect of chronic BAT activation and the mechanisms underlying BAT activation in humans to identify safe and efficacious lifestyle or pharmaceutical interventions that may activate BAT *in vivo* or induce the “browning” of the more abundant WAT. If the potential of *UCP1*-positive adipocytes to alter energy metabolism and expenditure in humans can be fully realized, BAT will likely emerge as a therapeutic target in the battle against obesity and diabetes.

Acknowledgments. The authors thank the study participants, and the nursing and administrative personnel at the Institute of Translational Sciences Clinical Research Center at the University of Texas Medical Branch (Galveston, TX). The authors also thank David Konkel and Sarah E. Toombs Smith, University of Texas Medical Branch, for editorial assistance. In addition, the authors thank Mohit Arora, Syed Habeebullah Husaini, Rene Przkora, Lily Kwatampora, and Alejandro Muñoz, University of Texas Medical Branch, for conducting the physical

assessment of the participants; Sam Jacob, Shriners Hospital for Children (Galveston, TX), for immunohistochemical analysis; Rajesh Kumar, University of Texas Medical Branch, for performing the PET/CT scans; Cynthia Locklin, Carrie Barone, and Aikaterini Iliadou, Shriners Hospital for Children, for their administrative and technical support; and Birgitte Andersen, Novo Nordisk, for analyzing the FGF21 plasma samples.

Funding. This study was conducted with the support of the Institute for Translational Sciences at the University of Texas Medical Branch (Galveston, TX); and was supported in part by a Clinical and Translational Science Award (UL1TR000071) from the National Center for Advancing Translational Sciences, the National Institutes of Health, American Diabetes Association grant 1-14-TS-35, Shriners Hospitals for Children grants 84090 and 85310, the John Sealy Memorial Endowment Fund for Biomedical Research grant 66992, Claude D. Pepper Older Americans Independence Center grant P30 AG024832, and the Sealy Center on Aging. M.C. is funded by the Onassis Foundation. S.E. was supported by Swedish Research Council grants 2010-3281 and 2012-1652, The Knut and Alice Wallenberg Foundation, Sahlgrenska University Hospital (LUA-ALF), European Union grant HEALTH-F2-2011-278373 (DIABAT), the Inga Britt and Arne Lundgren Foundation, the Söderberg Foundation, and the King Gustaf V and Queen Victoria Freemason Foundation. S.M.L. is funded by a Canadian Institutes of Health Research postdoctoral fellowship.

Duality of Interest. S.E. is a shareholder and consultant to Ember Therapeutics. No other potential conflicts of interest relevant to this article were reported.

Author Contributions. M.C. helped to design the study, and to perform the clinical trials, the statistical analysis, and the stable isotope analysis; wrote the initial draft of the manuscript; and critically reviewed the manuscript before publication. E.V. and E.B. helped to design the study and critically reviewed the manuscript before publication. C.P. and T.C. performed mitochondrial respiration analysis and critically reviewed the manuscript before publication. P.A. performed the adipose tissue biopsies, was responsible for the medical coverage of the studies, and critically reviewed the manuscript before publication. S.E. and M.E.L. designed and performed the gene expression experiments, and critically reviewed the manuscript before publication. M.K.S. analyzed hormone measurements from blood samples, designed and performed the immunohistochemistry experiments, and critically reviewed the manuscript before publication. S.M.L. performed the PET/CT scan analysis, and critically reviewed the manuscript before publication. N.M.H. helped to perform the clinical trials and critically reviewed the manuscript before publication. C.Y. helped to design the study and to perform the clinical trials, and critically reviewed the manuscript before publication. C.R.A. helped to perform the statistical analysis and critically reviewed the manuscript before publication. F.C. performed and supervised the PET/CT scans, and critically reviewed the manuscript before publication. H.H. designed and performed the immunohistochemistry experiments and critically reviewed the manuscript. L.S.S. helped to design the study and critically reviewed the manuscript before publication. M.C. and L.S.S. are the guarantors of this work and, as such, had full access to all the data in the study and take responsibility for the integrity of the data and the accuracy of the data analysis.

Prior Presentation. Parts of this study were presented in abstract form at the 74th Scientific Sessions of the American Diabetes Association, San Francisco, CA, 13–17 June 2014.

References

- Centers for Disease Control and Prevention. National Diabetes Fact Sheet [Internet], 2001. Atlanta, GA, Centers for Disease Control and Prevention. Available from <http://www.cdc.gov/diabetes/pubs/factsheet11.htm>. Accessed 10 March 2013
- Virtanen KA, Lidell ME, Orava J, et al. Functional brown adipose tissue in healthy adults. *N Engl J Med* 2009;360:1518–1525
- van Marken Lichtenbelt WD, Vanhomerig JW, Smulders NM, et al. Cold-activated brown adipose tissue in healthy men. *N Engl J Med* 2009;360:1500–1508

4. Cypess AM, Lehman S, Williams G, et al. Identification and importance of brown adipose tissue in adult humans. *N Engl J Med* 2009;360:1509–1517
5. Saito M, Okamatsu-Ogura Y, Matsushita M, et al. High incidence of metabolically active brown adipose tissue in healthy adult humans: effects of cold exposure and adiposity. *Diabetes* 2009;58:1526–1531
6. Ouellet V, Routhier-Labadie A, Bellemare W, et al. Outdoor temperature, age, sex, body mass index, and diabetic status determine the prevalence, mass, and glucose-uptake activity of ¹⁸F-FDG-detected BAT in humans. *J Clin Endocrinol Metab* 2011;96:192–199
7. Matsushita M, Yoneshiro T, Aita S, Kameya T, Sugie H, Saito M. Impact of brown adipose tissue on body fatness and glucose metabolism in healthy humans. *Int J Obes (Lond)* 2014;38:812–817
8. Cannon B, Nedergaard J. Brown adipose tissue: function and physiological significance. *Physiol Rev* 2004;84:277–359
9. Bartelt A, Bruns OT, Reimer R, et al. Brown adipose tissue activity controls triglyceride clearance. *Nat Med* 2011;17:200–205
10. Stanford KI, Middelbeek RJ, Townsend KL, et al. Brown adipose tissue regulates glucose homeostasis and insulin sensitivity. *J Clin Invest* 2013;123:215–223
11. Orava J, Nuutila P, Lidell ME, et al. Different metabolic responses of human brown adipose tissue to activation by cold and insulin. *Cell Metab* 2011;14:272–279
12. Ouellet V, Labbé SM, Blondin DP, et al. Brown adipose tissue oxidative metabolism contributes to energy expenditure during acute cold exposure in humans. *J Clin Invest* 2012;122:545–552
13. Orava J, Nuutila P, Noponen T, et al. Blunted metabolic responses to cold and insulin stimulation in brown adipose tissue of obese humans. *Obesity (Silver Spring)* 2013;21:2279–2287
14. Haman F, Péronnet F, Kenny GP, et al. Effect of cold exposure on fuel utilization in humans: plasma glucose, muscle glycogen, and lipids. *J Appl Physiol (1985)* 2002;93:77–84
15. International Standards Organization. Evaluation of thermal strain by physiological measurements [Internet]. ISO 9886:2004. Geneva, Switzerland, International Standards Organization. Available from http://www.iso.org/iso/home/store/catalogue_ics/catalogue_detail_ics.htm?csnumber=34110. Accessed 23 May 2011
16. Romijn JA, Coyle EF, Sidossis LS, Rosenblatt J, Wolfe RR. Substrate metabolism during different exercise intensities in endurance-trained women. *J Appl Physiol (1985)* 2000;88:1707–1714
17. Blaak EE, Wolffenbuttel BH, Saris WH, Pelsers MM, Wagenmakers AJ. Weight reduction and the impaired plasma-derived free fatty acid oxidation in type 2 diabetic subjects. *J Clin Endocrinol Metab* 2001;86:1638–1644
18. Mensink M, Blaak EE, Wagenmakers AJ, Saris WH. Lifestyle intervention and fatty acid metabolism in glucose-intolerant subjects. *Obes Res* 2005;13:1354–1362
19. Donga E, van Dijk M, van Dijk JG, et al. A single night of partial sleep deprivation induces insulin resistance in multiple metabolic pathways in healthy subjects. *J Clin Endocrinol Metab* 2010;95:2963–2968
20. Sidossis LS, Stuart CA, Shulman GI, Lopaschuk GD, Wolfe RR. Glucose plus insulin regulate fat oxidation by controlling the rate of fatty acid entry into the mitochondria. *J Clin Invest* 1996;98:2244–2250
21. DeFronzo RA, Tobin JD, Andres R. Glucose clamp technique: a method for quantifying insulin secretion and resistance. *Am J Physiol* 1979;237:E214–E223
22. Conte C, Fabbrini E, Kars M, Mittendorfer B, Patterson BW, Klein S. Multiorgan insulin sensitivity in lean and obese subjects. *Diabetes Care* 2012;35:1316–1321
23. Katz A, Nambi SS, Mather K, et al. Quantitative insulin sensitivity check index: a simple, accurate method for assessing insulin sensitivity in humans. *J Clin Endocrinol Metab* 2000;85:2402–2410
24. Gastaldelli A, Cusi K, Pettiti M, et al. Relationship between hepatic/visceral fat and hepatic insulin resistance in nondiabetic and type 2 diabetic subjects. *Gastroenterology* 2007;133:496–506
25. Borel AL, Nazare JA, Smith J, et al. Visceral and not subcutaneous abdominal adiposity reduction drives the benefits of a 1-year lifestyle modification program. *Obesity (Silver Spring)* 2012;20:1223–1233
26. Ferland M, Després JP, Tremblay A, et al. Assessment of adipose tissue distribution by computed axial tomography in obese women: association with body density and anthropometric measurements. *Br J Nutr* 1989;61:139–148
27. Paré A, Dumont M, Lemieux I, et al. Is the relationship between adipose tissue and waist girth altered by weight loss in obese men? *Obes Res* 2001;9:526–534
28. Børsheim E, Kien CL, Pearl WM. Differential effects of dietary intake of palmitic acid and oleic acid on oxygen consumption during and after exercise. *Metabolism* 2006;55:1215–1221
29. Cox RA, Mlcak RP, Chinkes DL, et al. Upper airway mucus deposition in lung tissue of burn trauma victims. *Shock* 2008;29:356–361
30. López M, Varela L, Vázquez MJ, et al. Hypothalamic AMPK and fatty acid metabolism mediate thyroid regulation of energy balance. *Nat Med* 2010;16:1001–1008
31. Boström P, Wu J, Jedrychowski MP, et al. A PGC1- α -dependent myokine that drives brown-fat-like development of white fat and thermogenesis. *Nature* 2012;481:463–468
32. Ma SW, Foster DO. Uptake of glucose and release of fatty acids and glycerol by rat brown adipose tissue in vivo. *Can J Physiol Pharmacol* 1986;64:609–614
33. Charkoudian N. Mechanisms and modifiers of reflex induced cutaneous vasodilation and vasoconstriction in humans. *J Appl Physiol (1985)* 2010;109:1221–1228
34. Jamerson KA, Julius S, Gudbrandsson T, Andersson O, Brant DO. Reflex sympathetic activation induces acute insulin resistance in the human forearm. *Hypertension* 1993;21:618–623
35. Gasparetti AL, de Souza CT, Pereira-da-Silva M, et al. Cold exposure induces tissue-specific modulation of the insulin-signalling pathway in *Rattus norvegicus*. *J Physiol* 2003;552:149–162
36. Hondares E, Iglesias R, Giralt A, et al. Thermogenic activation induces FGF21 expression and release in brown adipose tissue. *J Biol Chem* 2011;286:12983–12990
37. Lee P, Brychta RJ, Linderman J, Smith S, Chen KY, Celi FS. Mild cold exposure modulates fibroblast growth factor 21 (FGF21) diurnal rhythm in humans: relationship between FGF21 levels, lipolysis, and cold-induced thermogenesis. *J Clin Endocrinol Metab* 2013;98:E98–E102
38. Silva JE, Larsen PR. Potential of brown adipose tissue type II thyroxine 5'-deiodinase as a local and systemic source of triiodothyronine in rats. *J Clin Invest* 1985;76:2296–2305